8

Parameters Controlling Optical Feedback of Quantum-Dot Semiconductor Lasers

Basim Abdullattif Ghalib[1], Sabri J. Al-Obaidi[2] and Amin H. Al-Khursan[3,*]
[1]*Laser Physics Department, Science College for Women, Babylon University, Hilla,*
[2]*Physics Department, Science College, Al-Mustansiriyah University, Baghdad,*
[3]*Nassiriya Nanotechnology Research Laboratory (NNRL),*
Science College, Thi-Qar University, Nassiriya,
Iraq

1. Introduction

A simple model to describe the dynamics of a single mode semiconductor laser subject to a coherent optical feedback is proposed in 1980 by Lang and Kobayashi (LK). Feedback loop depends on external mirror and creates a passive external cavity, which is explicitly taken into account via the complex delayed electric field variable $E(t-\tau)$ fed back into the laser. The round trip time is the main feature of the LK model of the laser beam. The LK model has open the door to a very complex dynamics since the system phase space has infinite dimensions and sustain a chaotic regime [1]. Optical feedback consist of two subjects, coherent and incoherent feedback, depending on whether the coherence time of the laser light is larger or smaller than the delay time (τ) respectively [2]. There are five distinct regimes that are defined by the level of the feedback power ratio, this is discusses in section 2. The great importance for dynamics of semiconductor lasers with optical feedback is due to the potential applications of such lasers for secure communications by means of chaotic synchronization. External perturbations such as injected signal, feedback, or pump current modulation are required to achieve a chaotic output. From a practical point of view, optical feedback provided by a back reflecting mirror is one of the simplest ways to achieve chaotic oscillations from a semiconductor laser, even weak optical feedback leads to complex dynamics. In particular, it can sustain a chaotic regime of low-frequency fluctuations with sudden irregular intensity dropouts followed by a gradual intensity recovery [6].

To improve semiconductor laser performance, a nanoscale active region, in the form of two-dimensional quantum wells (one degree of freedom), one-dimensional quantum wires (two degrees of freedom), or zero-dimensional quantum dots (three degrees of freedom) are used [3]. Since quantum dot (QD) semiconductor materials have discrete energy subbands, one could expect symmetric emission lines, then the subject of great current interest is a sensitivity of QD semiconductor lasers to optical feedback [4]. QD lasers acquired more

* Corresponding Author

importance after significant progress in nanostructure growth by self-assembling technique. The first demonstration of a QD laser with low threshold current density was reported in 1994 [5]. A QD laser emits at wavelengths determined by the energy levels of the dots, rather than the bandgap energy. Thus, they offer the possibility of improved device performance and increased flexibility to adjust the wavelength. They have the maximum material and differential gain, at least 2-3 orders higher than QW lasers [6]. A QD laser is a semiconductor laser that uses QDs as the active laser medium in its light emitting region. Due to the tight confinement of charge carriers in QDs, they exhibit an electronic structure similar to atoms. Lasers fabricated from such an active media exhibit higher device performance compared to traditional semiconductor lasers based on bulk or quantum well active medium. Improvements in performance can appear in wide modulation bandwidth, while both lasing threshold, relative intensity noise, linewidth enhancement factor and temperature sensitivity are reduced. QD semiconductor lasers displays an interesting hybrid of atomic laser and standard quantum well semiconductor laser properties. Optical feedback containing very commonly in a wide variety of fields including biology, ecology and physics. In biology they occur in regulation and stabilization processes, e.g. blood cell-production, neural control and respiratory physiology and control of physiological systems (heart rate, blood pressure, motor activity) [7,8].

This chapter covers a review and a study of optical feedback in QD lasers. Section 2 reviews the characteristics of optical feedback regimes, while in section 3, the new rate equations for laser dynamics to describe the active region and Parameters used in the calculations. Section 4 includes a study of time delay effect on optical feedback at threshold current, phase and time delay.

2. Diode lasers with optical feedback

Optical feedback depends on several parameters and effects on the operating characteristics of a diode laser. One of these effects is the re-injection of a fraction of light into the laser diode after a time (τ) later delayed optical feedback. The optical feedback regimes consists of five distinct regimes defined by the level of the feedback power ratio. These regimes are depend on the internal parameters of the solitary diode laser, such as the linewidth enhancement factor, the diode dimensions and the facet coatings. They are:

Regime I corresponds to low feedback level were broadening or narrowing of the optical linewidth is observed depending on the feedback phase, the importance of this regime lies not in the manipulation of linewidths achievable, as greater control can be achieved in higher regimes. In regime II, two modes are observed do not simultaneously exist. As the feedback is increased towards regime III the mode hopping frequency and the mode splitting frequency increases. The transition to this regime from regime I is characterized by an observed line broadening. This regime overlaps regime I. The properties of regime III are single-mode operation and stability arises. The minimum linewidth mode has the best phase stability for this reason regime is inappropriate for most applications. This regime occupies only a very small value of feedback power ratios. Regime IV, which is observed for higher feedback levels, is associated with the coherence collapse this regime is useless for coherent communications. However, applications such as imaging or secure data transmission

require highly incoherent sources. In regime V, a stable emission with a narrow linewidth at high feedback levels. This regime is characterized by very narrow-linewidth stable single-mode low intensity noise operation. The coherence of the laser is regained. It operates as a long cavity laser with a short active region. Experimentally it is usually required to antireflection coat the diode laser front facet in order to reach this regime. Due to the strong feedback in this regime the system is also much less sensitive to additional reflections. The system operating in this regime is often referred to as an external cavity diode laser (ECDL) [12].

3. The rate equations for laser dynamics

In the QD laser, we considers a separate system for electrons and holes in the QD ground state (GS) and exited state (ES) which typically applies for the self-organized QDs in the $InN/In_{0.8}Al_{0.12}N/In_{0.25}Al_{0.75}N$ material system. The model used here is plotted in Fig. 1, where the various mechanisms that occurs in the laser cavity are abstracted. Our model recognizes between lifetimes according to carrier type (electron and hole) although their values are taken here the same for simplicity. First the carriers are injected in the wetting layer with rate I/q and relax in the dot. The carriers are captured in the ES with a rate $1/\tau_{c,w}^{e}, 1/\tau_{c,w}^{h}$ and from the ES to the GS with rate $1/\tau_{c,E}^{e}$, $1/\tau_{c,E}^{h}$. The carriers escape also from the GS back to the ES with rate $1/\tau_{e,G}^{e}, 1/\tau_{e,G}^{h}$ or from the ES back to the WL with rate $1/\tau_{e,E}^{e}$, $1/\tau_{e,E}^{h}$. The recombination processes of carriers from the WL and the QD confined states with rates $\tau_{r,w}^{e}\ \tau_{r,w}^{h}\ \tau_{r,E}^{e}\ \tau_{r,E}^{h}\ \tau_{r,G}^{e}\ \tau_{r,G}^{h}$, respectively. It is assumed that the stimulated emission can take place only due to recombination between the electrons and holes in the ES and GS. Then the rate equation system becomes:

$$\frac{dE_G}{dt} = -\frac{E_G}{2\tau_s} + \frac{1}{2}\Gamma g_G \upsilon_g(\rho_G^e + \rho_G^h - 1)E_G + \frac{1}{2}i\alpha(\rho_G^e + \rho_G^h)E_G + \frac{\gamma}{2}E_G(t-\tau) + R_{sp,GS} \tag{1}$$

$$\frac{dE_E}{dt} = -\frac{E_E}{2\tau_s} + \frac{1}{2}\Gamma g_E \upsilon_g(\rho_E^e + \rho_E^h - 1)E_E + \frac{1}{2}i\alpha(\rho_E^e + \rho_E^h)E_E + \frac{\gamma}{2}E_E(t-\tau) + R_{sp,ES} \tag{2}$$

$$\begin{aligned}\frac{d\rho_E^e}{dt} = &-\frac{\rho_E^e}{\tau_{r,E}^e} - \frac{\Gamma g_E \upsilon_g}{N_{QD}}(\rho_E^e + \rho_E^h - 1)\left|E_E\right|^2 - \frac{\rho_E^e(1-\rho_G^e)}{\tau_{c,E}^e} + \frac{\rho_G^e(1-\rho_E^e)}{\tau_{e,G}^e} \\ &- \frac{\rho_E^e}{\tau_{e,E}^e} + \frac{N_{w_e}}{N_{QD}\tau_{c,w}^e}\end{aligned} \tag{3}$$

$$\begin{aligned}\frac{d\rho_E^h}{dt} = &-\frac{\rho_E^h}{\tau_{r,E}^h} - \frac{\Gamma g_E \upsilon_g}{N_{QD}}(\rho_E^e + \rho_E^h - 1)\left|E_E\right|^2 - \frac{\rho_E^h(1-\rho_G^h)}{\tau_{c,E}^h} + \frac{\rho_G^h(1-\rho_E^h)}{\tau_{e,G}^h} \\ &- \frac{\rho_E^h}{\tau_{e,E}^h} + \frac{N_{w_h}}{N_{QD}\tau_{c,w}^h}\end{aligned} \tag{4}$$

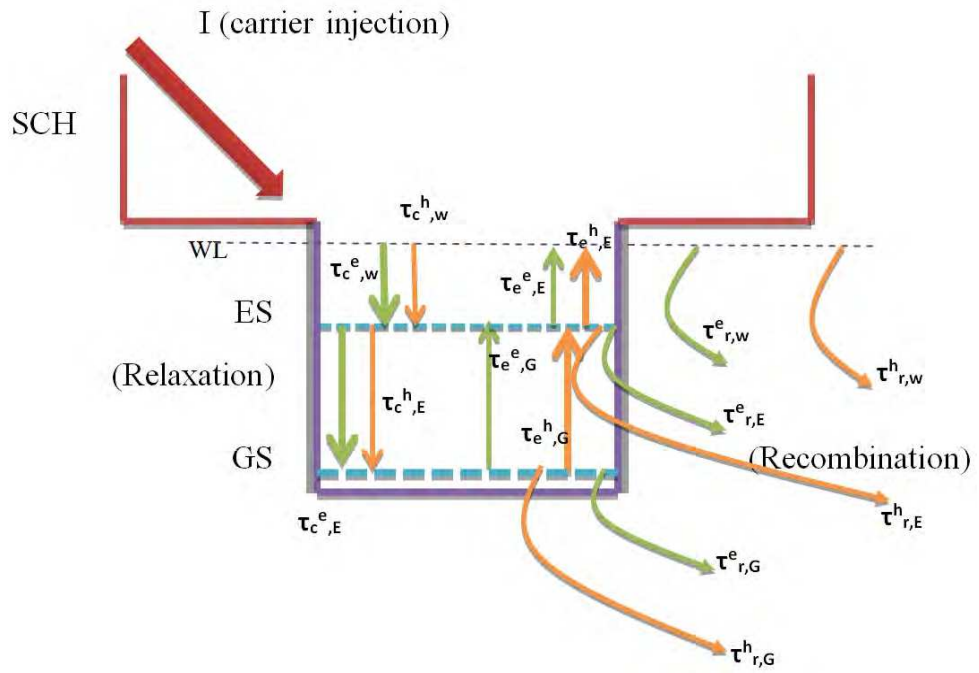

Fig. 1. Energy diagram of the active layer of the QD laser

$$\frac{d\rho_G^e}{dt} = -\frac{\rho_G^e}{\tau_{r,G}^e} - \frac{\Gamma g_G \upsilon_g}{N_{QD}}(\rho_G^e + \rho_G^h - 1)|E_G|^2 + \frac{\rho_E^e(1-\rho_G^e)}{\tau_{c,E}^e} - \frac{\rho_G^e(1-\rho_E^e)}{\tau_{e,G}^e} \tag{5}$$

$$\frac{d\rho_G^h}{dt} = -\frac{\rho_G^h}{\tau_{r,G}^h} - \frac{\Gamma g_G \upsilon_g}{N_{QD}}(\rho_G^e + \rho_G^h - 1)|E_G|^2 + \frac{\rho_E^h(1-\rho_G^h)}{\tau_{c,E}^h} - \frac{\rho_G^h(1-\rho_E^h)}{\tau_{e,G}^h} \tag{6}$$

$$\frac{dNw_e}{dt} = \frac{J_{c1}}{q} + \frac{\rho_E^e}{\tau_{e,E}^e} - \frac{N_{w_e}}{N_{QD}\tau_{c,w}^e} - \frac{N_{w_e}}{N_{QD}\tau_{r,w}^e} \tag{7}$$

$$\frac{dNw_h}{dt} = \frac{J_{c2}}{q} + \frac{\rho_E^h}{\tau_{e,E}^h} - \frac{N_{w_h}}{N_{QD}\tau_{c,w}^h} - \frac{N_{w_h}}{N_{QD}\tau_{r,w}^h} \tag{8}$$

Where E_G, E_E are complex amplitudes of electric field in the QD GS and ES, respectively, g_G, g_E are gain in GS and ES, respectively, Γ is the optical confinement factor, υ_g is the

group velocity, α is the linewidth enhancement factor, γ is the feedback level, $\rho_G^e, \rho_G^h, \rho_E^e, \rho_E^h$ are occupation probabilities in GS, ES for electrons (e) and holes (h) respectively, τ is the time delay, $R_{sp,GS}$, $R_{sp,ES}$ are the spontaneous emission rates in GS and ES, respectively. τ_S is the photon lifetime, N_{w_e}, N_{w_h} are the electron and hole carrier densities in the wetting layer, N_{QD} is the QD density. J_{c1}, J_{c2} are the current densities of electrons and holes, respectively. Equations (1-8) are solved numerically to describe the dynamics of the carrier densities in wetting layer for electrons and holes and the occupation probability in ground and exited states for electrons and holes.

4. Calculations and discussion

4.1 Effect of time delay on optical feedback

Figure 2 shows the time series of photon density in the GS. It shows a negligible value of the GS field. This can be results since the laser works at ES. The time series of the photon density in ES at three values of time delay is illustrated in Fig. 3(a)-(b) at the two values of threshold current ($1.5J_{th}$ and $4.5\ J_{th}$) respectively. From these figures one can show that the amplitude of the electric field in the ES increases with increasing current density. Approximately, as the current density doubles, ES photon density four times increases. On the other hand, the round trip delay time in the external cavity, τ, has a different effect. At shorter delay times, ES photon density four time increases, while further increment in the delay time doubles it. The laser delays by (3.5-4.5 ns) before the population inversion built then the relaxation oscillations built. The electric field amplitude is increased at longer round-trip external cavity delay time, i.e. longer external cavity length. The periodic oscillations are completely removed at shorter τ. This can be attributed to the observation [14] that these instabilities exhibited by QDs are related to long external cavity. Fig. 4 shows the time series of occupation probability of electrons in ES at different values of external cavity delay time τ. Fig. 5 shows the time evolution of electron and hole densities in WL. The same curve is obtained for all the three delay times. The symmetric rise of both densities results from taking the same parameters (at most) for both carriers, although the hole density somewhat higher than electron WL. The relaxation oscillations appears in the behavior of ES occupation while it is completely removed in the WL carrier behavior. This can be reasoned to the faster relaxation time from WL to ES and longer escape time to WL. Fig. 6 shows the three-dimensional (3D) plot of the ES photon density and GS occupation probability vs. time. It shows that the feedback oscillations of ES field raises when the GS occupation probability goes to unity.

4.2 Coherent and non-coherent optical feedback

The coherence and non-coherence are depends on the phase between incident and reflected waves by external cavity.

Figure 7 shows the ES photon density at three phases. The longer turn-on delay time is shown to increases with ϕ. When $\phi = 0$ the ES photon density takes a high value and the feedback oscillations are shown. When $\phi = \pi / 2$ the ES field amplitude is reduced and the oscillations appear at longer time. This reduction results from interference between forward

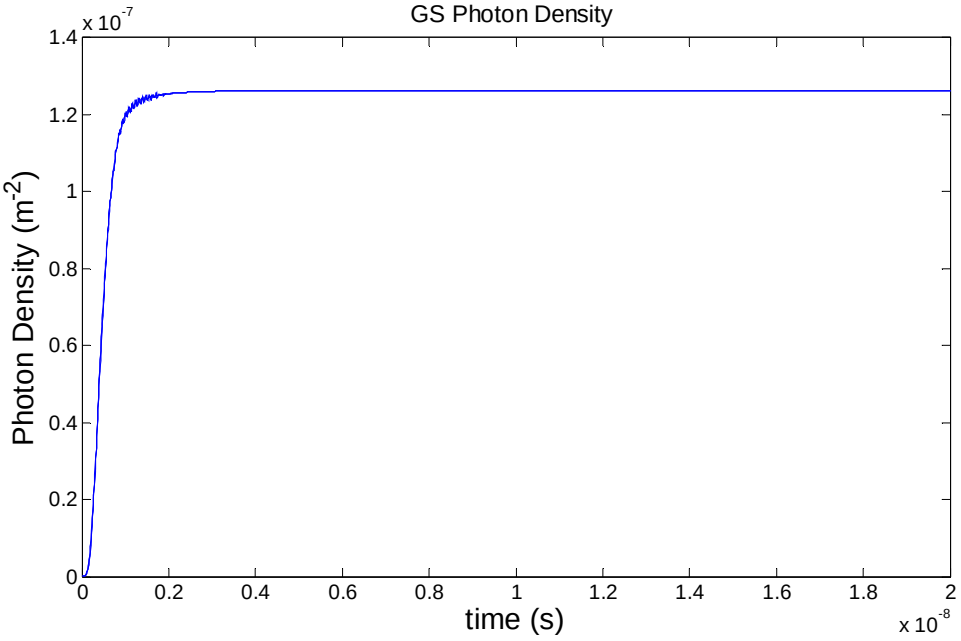

Fig. 2. Time variation of Photon density in GS when J_{c1}=1.5 J_{th},fi=0, α=2 andγ=0.025e12.

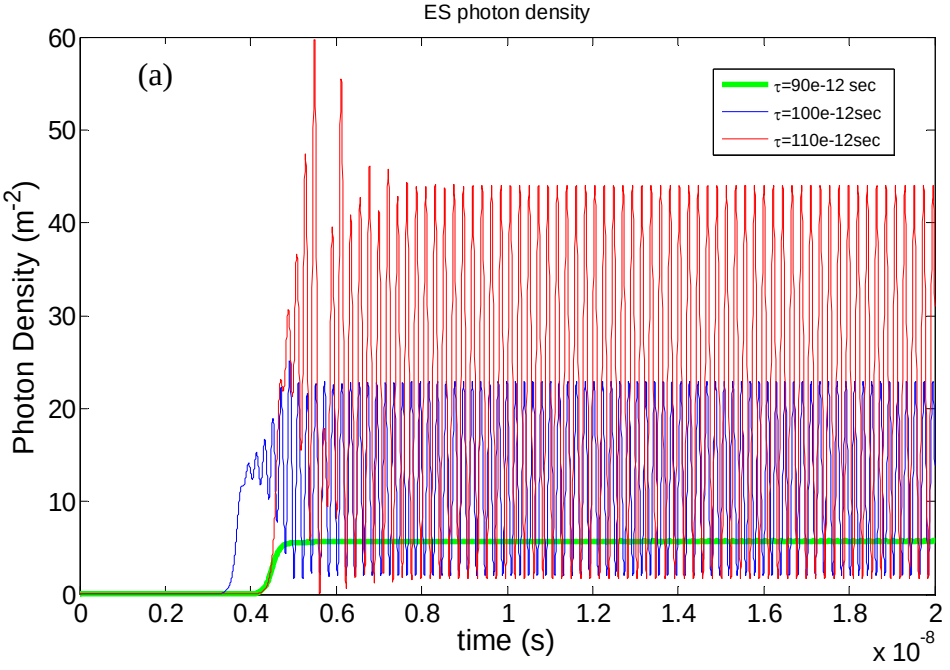

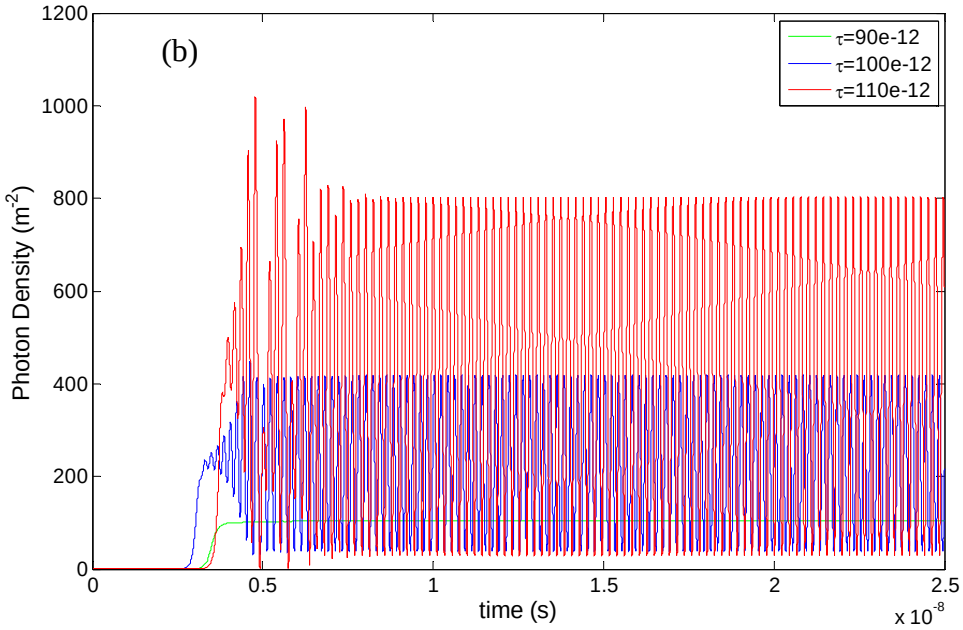

Fig. 3. Time variation of Photon density at three values of time delay when (a): J_{c1}=1.5 and J_{c1}=4.5 J_{th}. The simulation is done at the following parameters ϕ =0, α=2 and γ=0.025e12.

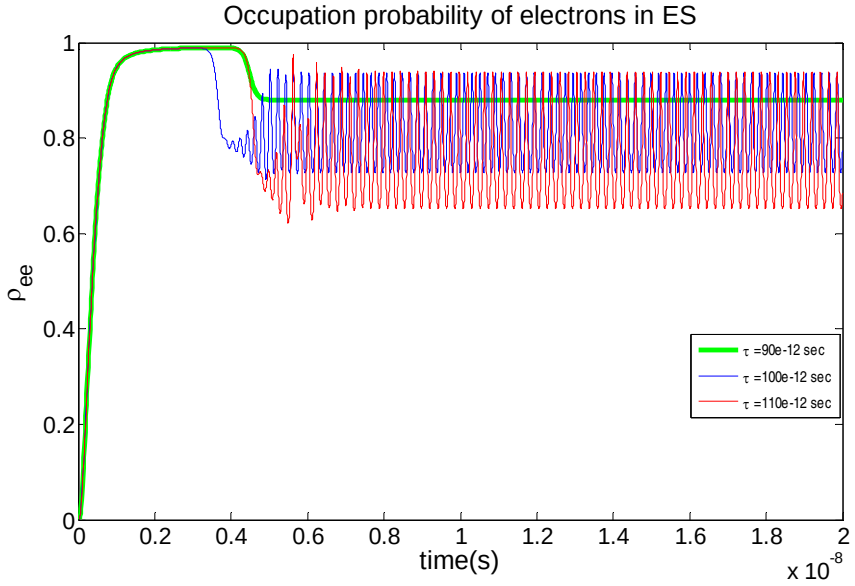

Fig. 4. Time series of electron occupation probability in ES at three values of time delay when J_{c1}=1.5 J_{th}, ϕ =0, α=2 and γ=0.025e12.

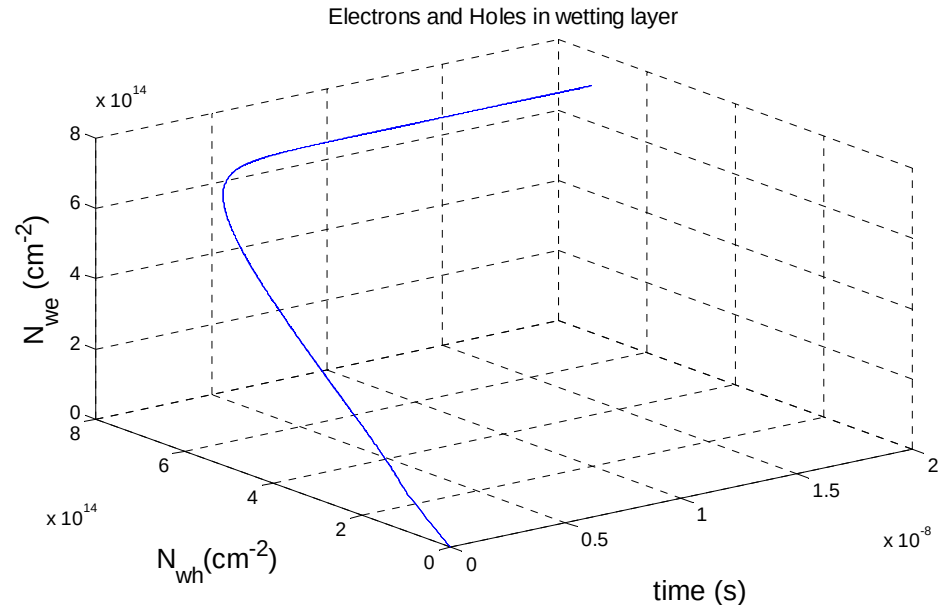

Fig. 5. 3D plot of WL electron and hole densities at J_{c1}=1.5 J_{th}, φ =0, α=2 and γ=0.025e12

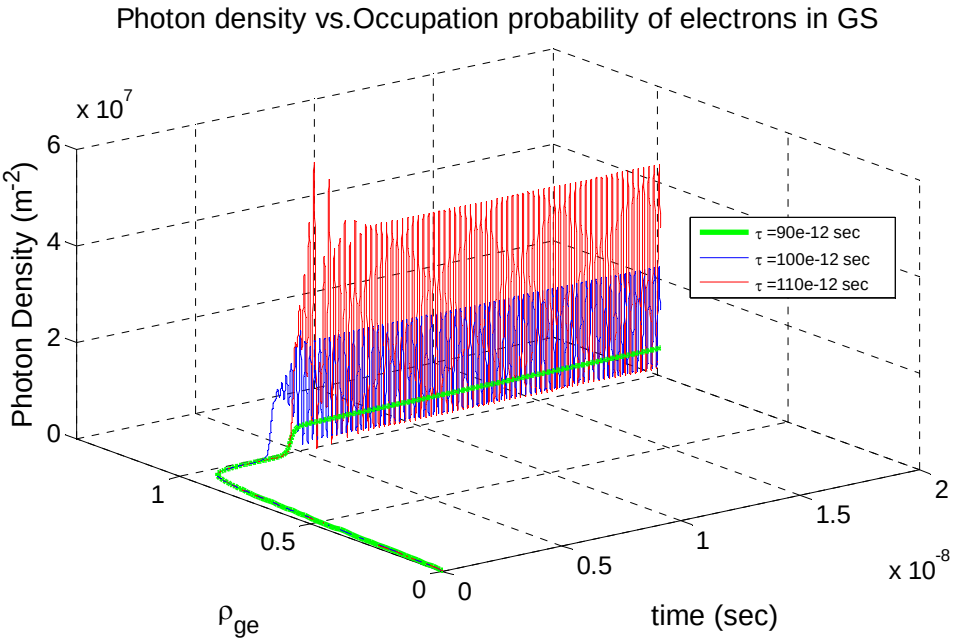

Fig. 6. 3D plot of photon density in ES, occupation probability in ES vs. time at three values of time delay when J_{c1}=1.5 J_{th}, ϕ =0, α=2 and γ=0.025e12.

and backward waves. When $\phi = \pi$ electric field is completely damped. This results from the destructive interference between the laser and the delay fields. To discuss this case let us study ES occupation probability at these phases. This is shown in Fig. 8. A point one must refer to here is the time spent before feedback oscillations appears. When the fields are constructively interfere ($\phi = 0$) the oscillations are appear earlier (~ after 5ns) then electron occupation is reduced. When $\phi = \pi / 2$, the interference have small effect where the oscillations appear at time (>1ns) and the reduction in electron occupation is small. In Fig. 9 a 3D plot of ES photon density vs. occupation probability of electrons and holes in ES. Although the occupation probability of electrons in ES goes to unity, the interference results in zero field at π-phase. This is also stressed by Fig. 9. Fig. 10 shows the 3D plot of ES photon density vs. occupation probability of (a): electrons and (b) holes in ES. Fig. 11 shows ES photon density vs. (a): electrons and (b): holes in wetting layer. One can discusses the case of $\phi = \pi$ by comparing Figs. 7 and 8. With increasing ϕ the carrier density increases while the photon density reduces. For small ϕ, the relaxation oscillations are high and depletes the carrier density where the laser gain attains. For $\phi = \pi$ case the laser turns off, but due to current injection the carrier density increases until the gain is achieved again then, the laser turns on and undergoes relaxation oscillations. The memory of similar earlier events is retained [15] within the external cavity and reinjected into the laser cavity. Finally an equilibrium state is achieved. Depending on this, one can also relates the longer turn-on delay time with increasing ϕ shown in Fig. 7 to the carrier depletion occurs with increasing incoherence.

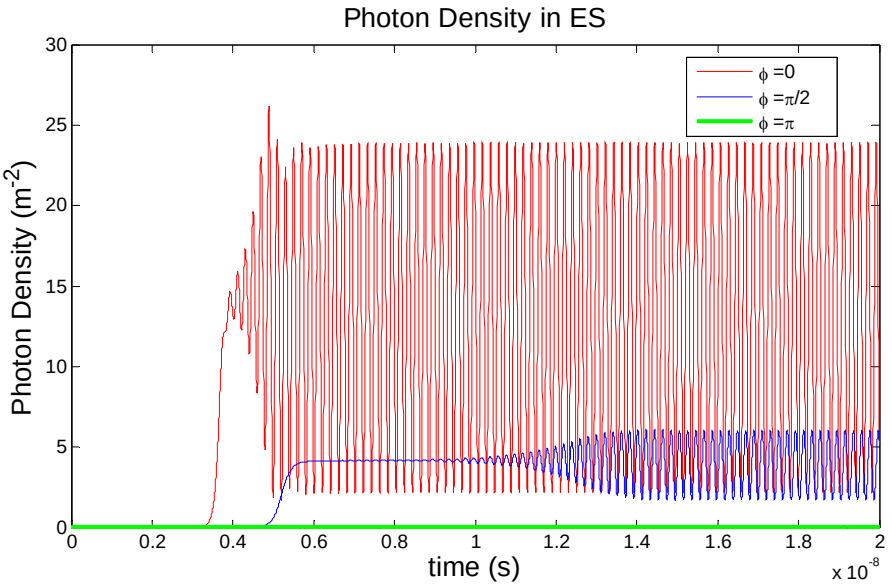

Fig. 7. Time series of ES photon density at three phase values when J_{c1}=1.5 J_{th}, $\tau = 100ps$, α=2 and γ=0.025e12.

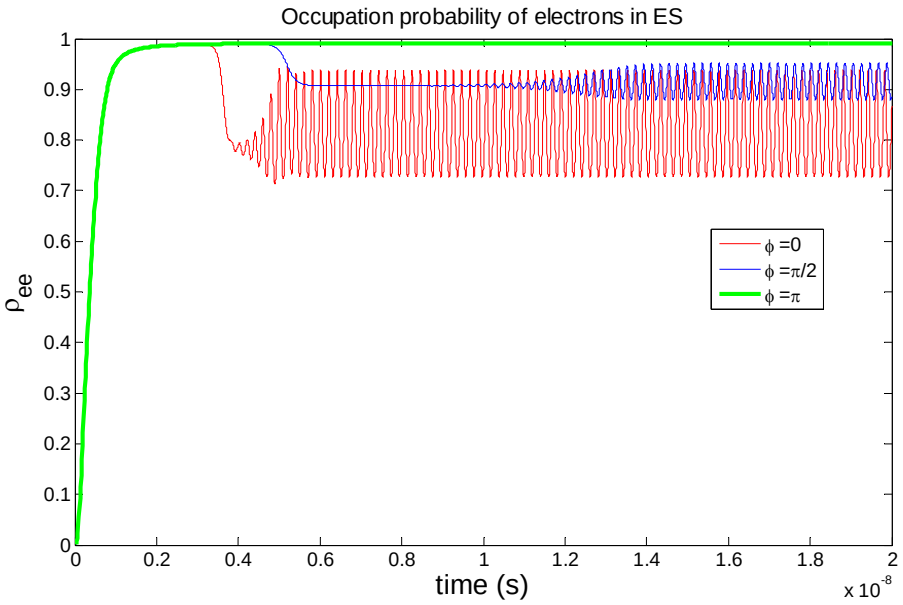

Fig. 8. Time series of occupation probability of ES electrons at three values of ϕ when J_{c1}=1.5 J_{th}, $\tau = 100ps$, α=2 and γ=0.025e12.

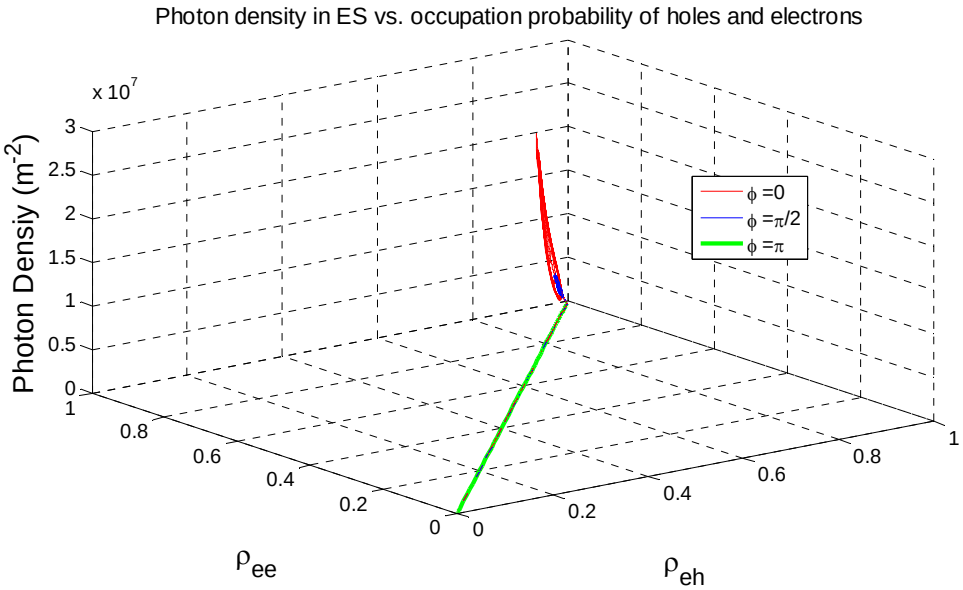

Fig. 9. 3D plot of ES photon density vs. occupation probability of electrons and holes in ES at three values of ϕ when J_{c1}=1.5 J_{th}, $\tau = 100ps$, α=2 and γ=0.025e12.

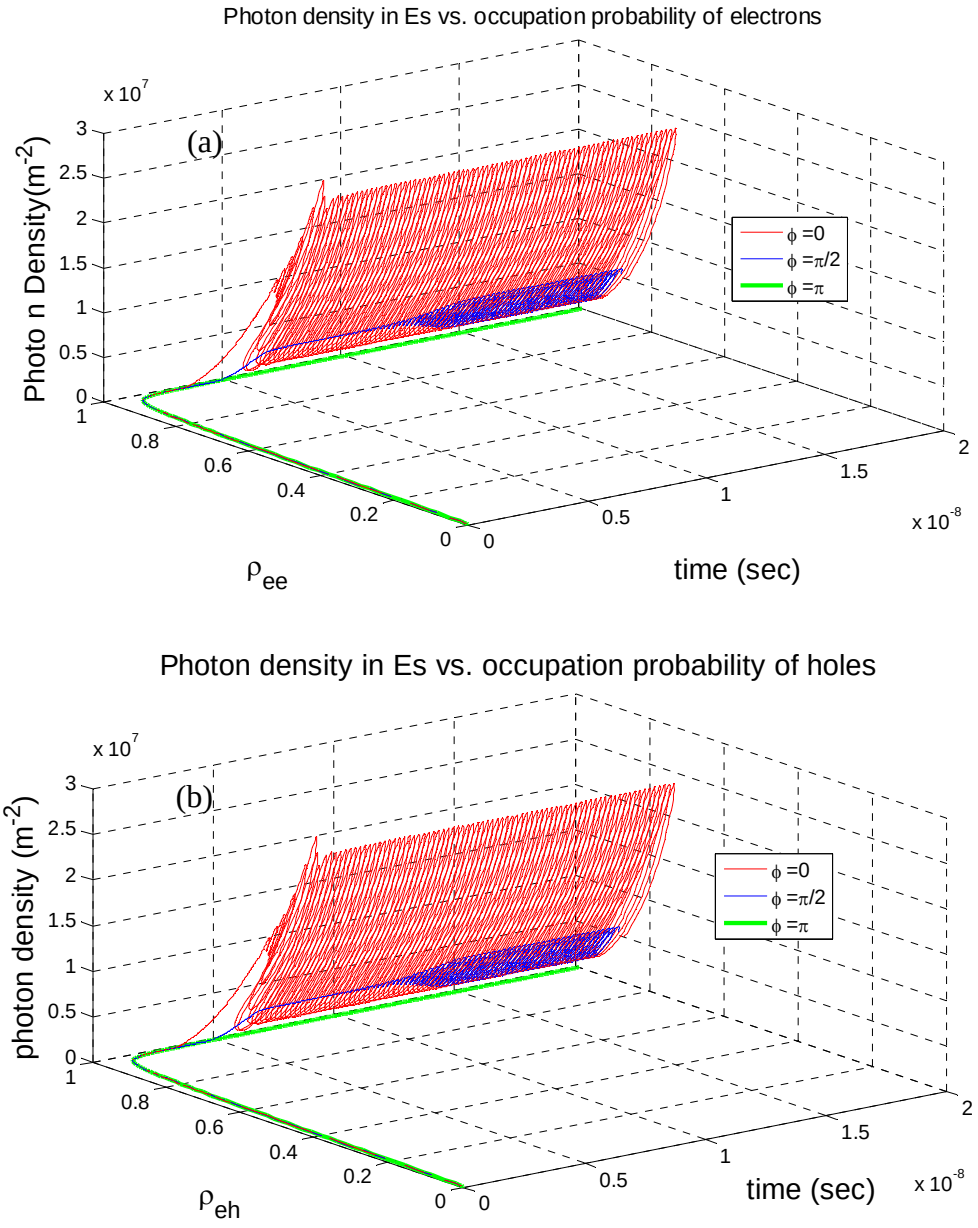

Fig. 10. 3D plot of electric field in ES vs. occupation probability of (a): electrons and (b) holes in ES at three values of ϕ when J_{c1}=1.5 J_{th}, $\tau = 100ps$, α=2 and γ=0.025e12.

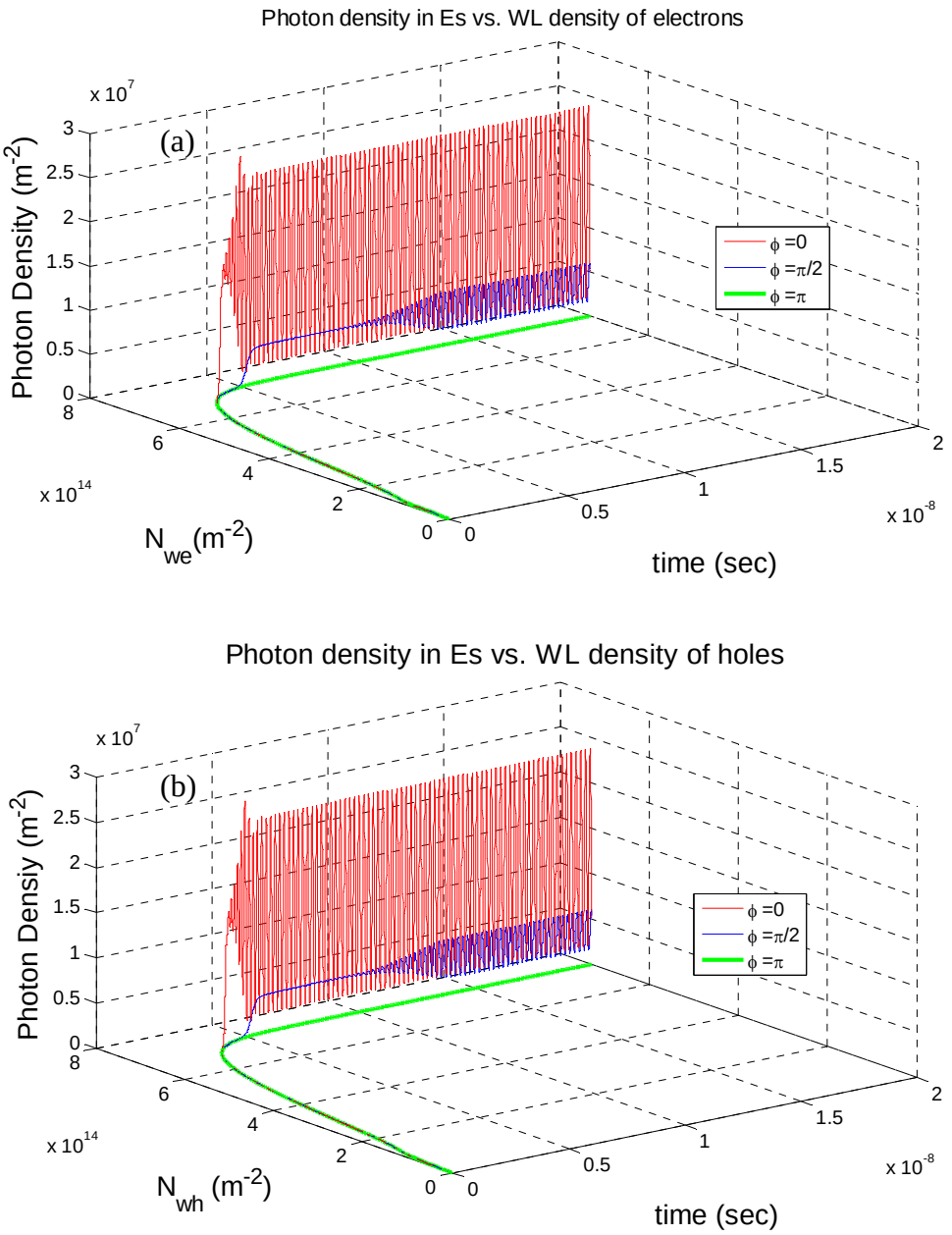

Fig. 11. 3D plot of electric field in ES vs. (a): electrons and (b): holes in wetting layer at three values of φ when *Jc1=1.5 Jth*,τ = 100*ps* , α=2 and γ=0.025e12.

Parameter	Symbol	Value	Unit
Recombination lifetime of electrons in GS	$\tau_{r,G}^{e}$	0.4	ns
Recombination lifetime of holes in GS	$\tau_{r,G}^{h}$	0.4	ns
Recombination lifetime of electrons in ES	$\tau_{r,E}^{e}$	0.4	ns
Recombination lifetime of holes in ES	$\tau_{r,E}^{e}$	0.4	ns
Recombination lifetime of electronsin WL	$\tau_{r,w}^{e}$	1000	Ps
Recombination lifetime of holes in WL	$\tau_{r,w}^{h}$	1000	Ps
Carrier capture time of electronsin WL	$\tau_{c,w}^{e}$	3	ns
Carrier capture time of holesin WL	$\tau_{c,w}^{h}$	3	ns
Carrier escape time of electrons from ES to WL	$\tau_{e,ES}^{e}$	1000	ps
Carrier escape time of holes from ES to WL	$\tau_{e,ES}^{h}$	1000	ps
Carrier relaxation time of electrons from GS to ES	$\tau_{e,GS}^{e}$	1.2	Ps
Carrier relaxation time of holes from GS to ES	$\tau_{e,GS}^{h}$	1.2	ps
Carrier relaxation time of electrons from ES to GS	$\tau_{c,ES}^{e}$	0.16	Ps
Carrier relaxation time of holes from ES to GS	$\tau_{c,ES}^{h}$	0.16	Ps
Optical confinement factor	Γ	$7*10^{-3}$	
Density of QDs	N_{QD}	$5*10^{14}$	cm^{-2}
Laser length	L	$2*10^{-3}$	cm
Effective thickness of the active Layer	L_w	$0.2*10^{-6}$	cm

Table 1. Parameters used in calculations.

5. Conclusions

The feedback in quantum dot lasers is discussed. The rate equations model using the delay differential equations is stated and solved numerically to elucidate the behavior of different states in the quantum dot laser. excited states in quantum dot is shown to have an important effect on the feedback. Effect of decoherence is studied and is shown to delays the laser field due to carrier depletion.

6. References

[1] D. Pieroux and P. Mandel, "Low-frequency fluctuations in the Lang- Kobayashi equation", Physical Review E 68, (2003): 036204.

[2] J. M. Pol, " Semiconductor Laser Dynamics Compound-cavity", Ph.D. University of Balears (2002).

[3] E. Kapon, D. M. Hwang and R. Bhat, "Stimulated Emission in Semiconductor Quantum Wire Heterostructures," Phys. Rev. Lett., 63, No.4 (1989): 430.

[4] D. O`Brien, S. P. Hegarty and G. Huyet and A. V. Uskov, "Sensitivity of quantum-dot semiconductor lasers to optical feedback," Optics Letters, 29, No.10 (2004): 1072.

[5] M.Grundmann, D. Bimberg, V. M. Ustinov, S. S. Ruvimov, M. V. Maximov, P. S. Kop'ev, Zh. I. Alferov, U. Richter, P. Werner, U. Gosele, H. J. Kirstaedter, N. N. Ledentsov. "Low threshold, large to injection laser emission from (InGa)As quantum dots," Electron. Lett., 30 (1994): 1416.

[6] M. Datta and Z. Wasiczko Dilli, "Quantum Dot Lasers", (CambridgeUniversity Press, Cambridge, 1997) 11.

[7] D. Bimberg, M. Grundmann, and N. N. Ledentsov, "Quantum Dot Heterostructures", (John Wiley & Sons Ltd., New York, 1999).

[8] M. Kuntz, N. N. Ledentsov, D. Bimberg, A. R. Kovsh, V. M. Ustinov, A. E. Zhukov and Y. M. Shernyakov, "Spectrotemporal response of 1.3 mm quantum-dot lasers," Appl. Phys. Lett. 81, No.20 (2002): 3846.

[9] I. V. Koryukin and P. Mandel, "Dynamics of semiconductor lasers with optical feedback: Comparison of multimode models in the low-frequency fluctuation regime," Physical Review A 70 (2004): 053819.

[10] S. B. Kuntze, B. Zhang, L. Pavel, "Impact of feedback delay on closed- loop stability in semiconductor optical amplifier control circuits," J. Lightwave Technology, 27, No.9 (2009): 1095.

[11] J. L. Chern, K. Otsuka, and F. Ishiyama, "Coexistence of Two Attractors in Lasers with Delayed Incoherent Optical Feedback," Opt. Comm. 96, (1993): 259.

[12] R. W. Tkach and A. R. Chraplyvy, "Regimes of feedback effects in 1.5μm distributed feedback lasers," J. Lightwave Technology, LT-4, (1986): 1655.

[13] A. V. Uskov. D. O'Brien, S. P. Hegarty, and G. Huyet, "Sensitivity Of quantum-dot semiconductor lasers to optical feedback," Optics Letters, 29, No.10 (2004): 1027.

[14] E. A. Viktorov, P. Mandel and G. Huyet, "Long-cavity quantum dot laser," Optics Letters, 32, (2007): 1268.

[15] R. Ju and P. Spencer, "Dynamic Regimes in Semiconductor Lasers Subject to Incoherent Optical Feedback," J. Lightwave Technology, 23 (2005): 2513.

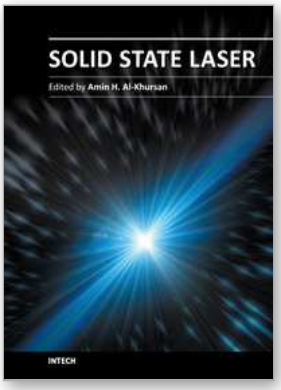

Solid State Laser

Edited by Prof. Amin Al-Khursan

ISBN 978-953-51-0086-7
Hard cover, 252 pages
Publisher InTech
Published online 17, February, 2012
Published in print edition February, 2012

This book deals with theoretical and experimental aspects of solid-state lasers, including optimum waveguide design of end pumped and diode pumped lasers. Nonlinearity, including the nonlinear conversion, up frequency conversion and chirped pulse oscillators are discussed. Some new rare-earth-doped lasers, including double borate and halide crystals, and feedback in quantum dot semiconductor nanostructures are included.

INTECH
open science | open minds

InTech Europe
University Campus STeP Ri
Slavka Krautzeka 83/A
51000 Rijeka, Croatia
Phone: +385 (51) 770 447
Fax: +385 (51) 686 166
www.intechopen.com

InTech China
Unit 405, Office Block, Hotel Equatorial Shanghai
No.65, Yan An Road (West), Shanghai, 200040, China
中国上海市延安西路65号上海国际贵都大饭店办公楼405单元
Phone: +86-21-62489820
Fax: +86-21-62489821